

Thomas Olsen

Keratometry

What is the corneal power? Most clinicians will ask for the “K-reading” neglecting the fact that the keratometer does not measure the power directly. What is measured is the size of the Purkinje I image reflected from the front surface of the cornea in a para-central ring of 3 mm or so and from this the radius of curvature is calculated [1].

The measurement of corneal curvature is among the oldest disciplines in ocular biometry. Since the front corneal surface acts as a convex mirror, it is a straightforward task to measure the curvature by measuring the magnification of that mirror. This is the principle of all Placido-based keratometers and topographers. We will have a detailed look at the conditions for this measurement.

The dioptric power of a reflecting convex mirror is given by

$$F_m = -\frac{2n}{r} \quad (14.1)$$

where F_m is reflective power of mirror (corneal surface) in diopters and r is radius of curvature in meters. For example, if $r = 7.8$ mm and $n = 1$ (air), then F_m becomes -260 D. This corresponds to a focal length of about -3.9 mm ($=1/-260$). In

other words, a distant object (e.g., the mires of the keratometer) will be focused 3.9 mm behind the cornea. Since the magnification is inversely related to power (or directly proportional to curvature), one can get a curvature measurement from the magnification of the mires observed in the reflection by the corneal surface.

The size of the object reflected by the cornea determines the effective area of the cornea to be measured. A large object means a larger zone to be examined and vice versa. There is a trade-off here as decreasing the diameter will increase the measurement error. Standard keratometers often use bright ring objects to be reflected in a 3 mm diameter ring on the cornea. It is important to note that in this way keratometry does not measure the very central power of the cornea. To get the full picture of the cornea, it is often better to use Placido keratoscopy or topography by which the entire area of optical interest can be examined (Fig. 14.1).

One may ask why we do not use topography as the standard rather than keratometry which only gives the radius in a small area? The reading of the keratometer is however often more accurate than the topographer because of automated alignment control and other measures to ensure a consistent reading. It is also a good idea regularly to check the reading against calibrated steel balls or other spheres with a known curvature.

T. Olsen (✉)
Aros Private Hospital, Aarhus N, Denmark

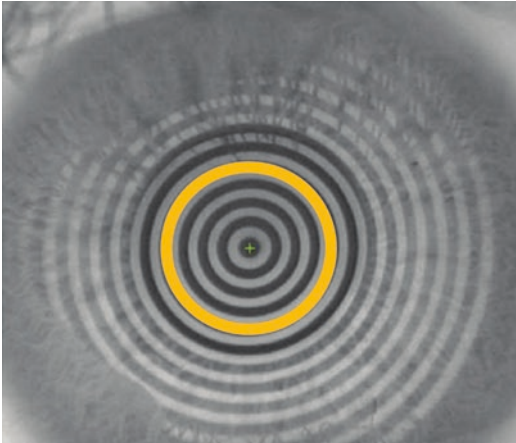


Fig. 14.1 Photokeratometry of the normal cornea. The standard keratometer measures the image size in the standard 3 mm ring zone (ring insert)

Instrumentation

The world's first keratometer was built by Herman Helmholtz in 1854, just a couple of years after he invented the ophthalmoscope. The optical principle of the Helmholtz keratometer was very advanced and allowed high precision measurements to be taken that was independent of the distance between the patient's eye and that of the observer. The optical principle was later implemented in the "ophthalmometer" manufactured by the Zeiss company in 1950—about 100 years after Helmholtz disclosed his principle. A clever arrangement was the use of image doubling through plane-parallel plates (compensating for eye movements) so that the observer would have to superimpose two images projected to infinity by adjusting a beam splitter that would eventually translate into radius of curvature.

Later in the eighteenth century, Émile Javal and Hjalmar Schiötz designed a keratometer that gained widespread use because of its simplicity. Rather than doubling the image, the Javal instrument doubles the object and the task of the observer is to move the distance between the two mire objects so that they will align through the eyepiece. The Bausch & Lomb keratometer produced from 1932 onwards was also based on this concept. The Javal type instrument was mainly

meant to measure astigmatism and was less accurate than the Helmholtz model because the measuring result depends on the distance between the patient's eye and the instrument.

Modern keratometers have shifted from manual to automated principles using LED (mostly infrared) as test mires and CCD to capture the image. The sensitivity of modern CCDs is so high that the exposure time can be kept sufficiently low so that the effect of eye movements is minimized. For the same reason, there is no need for image doubling and many mechanical features have been replaced by electronic processing and image analysis.

At the time of development of the early keratometers, the clinical interest was focused on astigmatism measurement and contact lens fitting. Little interest was given to the exact translation of radius into dioptric power. Of course, this is the most important subject of IOL power calculation for which accuracy is the top priority.

A detailed description of modern instrumentation is beyond the scope of this chapter.

The Calculation of Power from Curvature

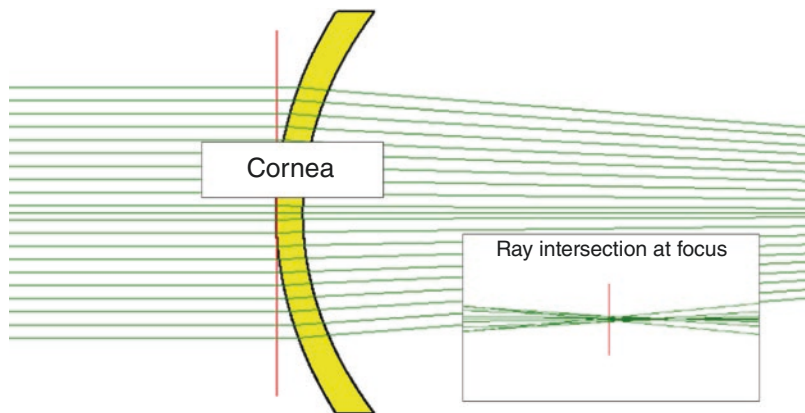
The refractive power of a single spherical surface is given by

$$F = \frac{n_2 - n_1}{r} \quad (14.2)$$

where F is refractive power of the surface, n_1 and n_2 are the refractive indices of the first and second medium, respectively, and r is radius of curvature in meters. For example (front surface of the cornea), if $r = 7.7$ mm, $n_1 = 1$ (air), $n_2 = 1.376$ (cornea), then F becomes +48.83 D. For example (back surface of the cornea), if $r = 6.8$ mm, $n_1 = 1.336$ (aqueous), $n_2 = 1.376$ (cornea), then F becomes -5.88 D.

Now, the cornea is not a single surface but rather two surfaces that combine to produce the total refraction (Fig. 14.2). The paraxial, refractive power of two spherical surfaces in combination is given by

Fig. 14.2 The refraction of the cornea occurs at the front and back surface



$$F_{12} = F_1 + F_2 - \frac{D}{n} * F_1 * F_2 \quad (14.3)$$

where F_{12} is total refractive power of the two surfaces, F_1 and F_2 are refractive power of the first and second surface, respectively, D is distance between the two surfaces, and n is refractive index between the two surfaces. Equation (14.3) is also called the paraxial formula for the combination of two surfaces or the “thick-lens equation.”

The dark horse is the curvature of the posterior surface of the cornea, which is not directly visible from the outside. So, for anterior keratometry to give a meaningful diopter reading for the whole cornea, certain assumptions need to be made.

One such assumption might be to use a schematic eye as a model for the ratio between the front and back surface of the cornea. The front and back corneal curvature of the Gullstrand exact schematic eye are 7.7 and 6.8 mm, respectively, giving a “Gullstrand ratio” between the front and back curvature of $6.8/7.7 = 0.883$. (Modern Scheimpflug and OCT techniques tend to give a slightly lower values—typically 0.83 or 0.84—but we will come back to that later.) If we assume a Gullstrand ratio of 0.883, then it is a straightforward calculation to calculate the total refractive power of the standard cornea (0.5 mm thick) as

$$F_{12} = 48.83 - 5.88 + \frac{0.0005}{1.376} * 48.8 * 5.9 = 43.05 \text{ D} \quad (14.4)$$

Now, if we want this value to be read directly from the anterior curvature, we can try and simulate what the assumed index of refraction should be using the single surface model (Eq. 14.2). Thus, if we substitute the power and curvature and solve for the assumed refractive index of the cornea, we get:

$$43.05 = \frac{n-1}{7.7} \geq n = 43.05 * 7.7 + 1 = 1.3315 \quad (14.5)$$

Note that this value is lower from the value of 1.3375 used by standard keratometry. The difference amounts to about 0.8 D higher reading of the standard keratometer as compared to the Gullstrand cornea!

Why has index 1.3375 become the standard? The reason seems to be from early days of instrument making where the exact corneal power was of less clinical interest than the astigmatism which can be found as the difference between the flat and the steep meridian. For practical purposes, the value of 1.3375 means that a corneal curvature of 7.5 mm would give a reading of 45 D so it was easy to check the calibration of the instrument. In 1909, Gullstrand wrote *Diese Zahl wurde aus technischen Gründe gewählt, damit 45 Dptr einem Radius von 7.5 mm entsprechen zollte* [2]. (“This number was chosen for technical reasons, so that 45 D corresponded to a radius of 7.5 mm.”)

For realistic IOL power calculation, it is very important that the power of the cornea is correct. If we start the process by making an error of 1.0 D, we will have to correct it at the end to avoid off-set errors.

Asphericity and Ray Tracing

The above considerations are valid in the paraxial domain with the fundamental assumption that all angles “*i*” are so small that $\sin(i) = i$. As we move away from the central axis, this assumption is no longer valid; therefore, paraxial imagery cannot be used to describe the effective refraction that includes higher order aberrations like spherical aberrations.

The cornea is not a spherical surface but rather an ellipsoid that tends to flatten at the periphery thereby decreasing the spherical aberration, but not all of it. Many studies have been published on the spherical aberration of the cornea, and many modern clinical Scheimpflug or OCT instruments offer comprehensive analysis of the higher order aberrations, including the spherical aberrations. To demonstrate the effect of the corneal asphericity, the author uses the values obtained by Dubbelman [3] for the normal cornea (Table 14.1).

The asphericity has some implications for the measurements of corneal curvature. As mentioned above, the standard keratometer is actually blind to the very center of the cornea—which is the steepest—but uses a ring zone of about 3 mm (often called the SimK) depending on the device. The 3 mm diameter of the cornea corresponds to about 11–12° of the cornea, assuming a normal curvature of 7.7 mm.

A relevant question is how much error the 3 mm zone reading deviates from the central zone? For this study, we can model the corneal shape as a conic section and use the abundance of

mathematical methods to describe conical sections. Baker (1943) [4] described a simple formula that is useful for ray tracing:

$$y^2 = 2rx - px^2 \tag{14.6}$$

where *x* and *y* are the coordinates of the conic surface with origin in (0, 0), *r* = apical radius and *p* is a constant describing the shape. For $0 < p < 1$, the shape is a prolate. Another term commonly used is the *Q*-value defined as $Q = p - 1$. Typical values for the front corneal surface range from -0.2 to -0.4 which means the shape of the cornea is a prolate.

Now, assuming an apical radius of 7.7 mm and a *Q*-value of -0.18, we can calculate what the sagittal radius of the cornea—the one that is measured by the keratometer—will be as a function of displacement from the axis (Fig. 14.3). From this graph, the keratometer reading of a standard 3 mm diameter (green rectangle) would give a 7.72 mm radius as compared to 7.70 at the apex. This corresponds to a 0.12 D difference. Of course, this difference may be higher when the cornea is abnormal, i.e., with a post-LASIK or a keratoconus cornea.

This asphericity reduces the spherical aberration, but not all of it. Depending on the contribution from the lens, the total optics of the eye typically shows some spherical aberration which is dependent on the pupil size. This is responsible for the night myopia found in many individuals.

What does the asphericity of the cornea mean for the effective power of the cornea? This can be studied by exact ray tracing that does not have the limitations of paraxial imagery. The only assumption of exact ray tracing is Snell’s law:

$$\frac{\sin \theta_1}{\sin \theta_2} = \frac{n_2}{n_1} \tag{14.7}$$

where *n*₁ and *n*₂ are the refractive indices of medium 1 and 2, respectively, and θ_1 and θ_2 are the incident angles in medium 1 and the outgoing angle in medium 2, respectively.

In the following ray tracing experiments, we again assume the cornea model of Dubbelman with a conic coefficient of the cornea of -0.18 and -0.38 for the anterior and posterior surface, respectively (Table 14.1). Assuming an

Table 14.1 Dubbelman model for corneal asphericity

Dubbelman cornea model	Apical radius (mm)	<i>Q</i> -value
Cornea front	7.70	-0.18
Cornea back	6.48	-0.38

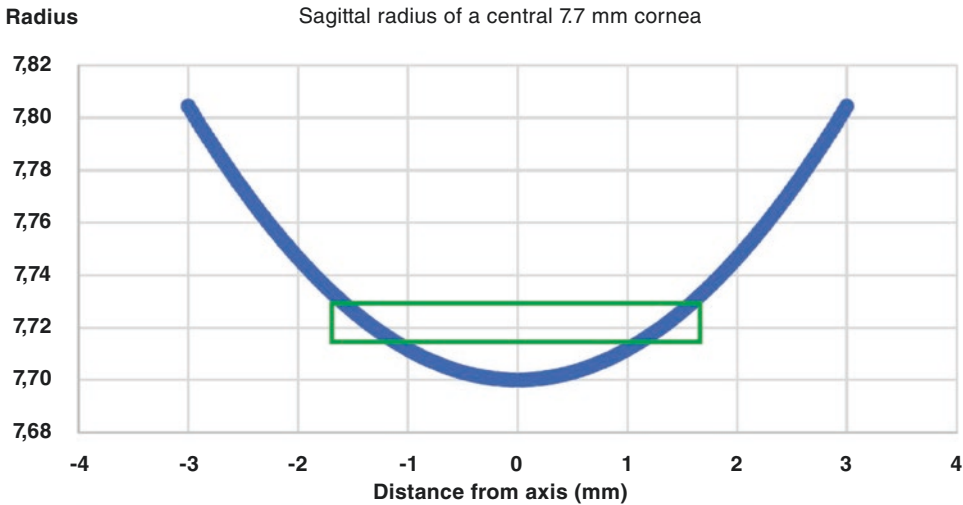


Fig. 14.3 Sagittal radius of cornea as a function of distance from axis. The rectangle insert illustrates the keratometer area of measurement

anterior apical radius of 7.70 mm and a posterior radius of 6.47 mm (Dubbelman's mean value) and a thickness of 0.5 mm, we trace a high number of rays through the cornea (Fig. 14.4) and look for the focus, which may be defined as the point on the axis having the least spread or the highest point spread function (PSF) (Fig. 14.5). Once the focal distance " d " has been found, we can then calculate the corresponding power as $F = n/d$ where n is the refractive index of aqueous (1.336).

To study the effect of pupil size, experiments were made with pupil sizes varying between 0 and 6 mm. As expected, the effective power of the cornea was found to increase with larger pupil diameter. The spherical aberration can be found as the difference between the central power and the power at the larger pupil. For normal pupil size (3 mm), the spherical aberration is within 0.25 D. To reach more than 0.5 D, the pupil size should be more than 5 mm.

All of the above concerns the normal cornea and ways to predict the effective corneal power. To study the effect of varying degrees of asphericity, we may conduct experiments varying the Q -values of the cornea around the normal value (Fig. 14.6). As can be seen in the figure, the spherical aberration is linearly correlated with

the Q -value of both surfaces. However, the posterior cornea has a much lower influence.

As can be seen, the effective corneal power is very much influenced by the shape of the cornea. Simply taking a K-reading is only part of the story. We must consider the total area of refraction and most preferably use ray tracing, nomograms or other techniques to get the effective corneal power to be used in the IOL power calculation.

According to the author's own experience using Scheimpflug photography (Oculus Pentacam HR), the normal Q -values range from -0.80 to $+0.65$ (mean value -0.05 with a standard deviation of 0.23) and from -0.90 to $+0.85$ (mean value -0.34 with a standard deviation of 0.21) of the front and back corneal surfaces, respectively. For comparison, post-myopic LASIK corneas may have higher Q -values (higher spherical aberration) of the front surface, ranging from -1.00 to $+3.1$ (mean value of 0.60 with a standard deviation of 0.80, illustrating the larger spread) and mean value -0.24 ranging from -0.90 to $+0.40$ (mean value -0.24 with a standard deviation of 0.22) of the back corneal surface.

An advantage of exact ray tracing is that it is possible to study the image quality by means of

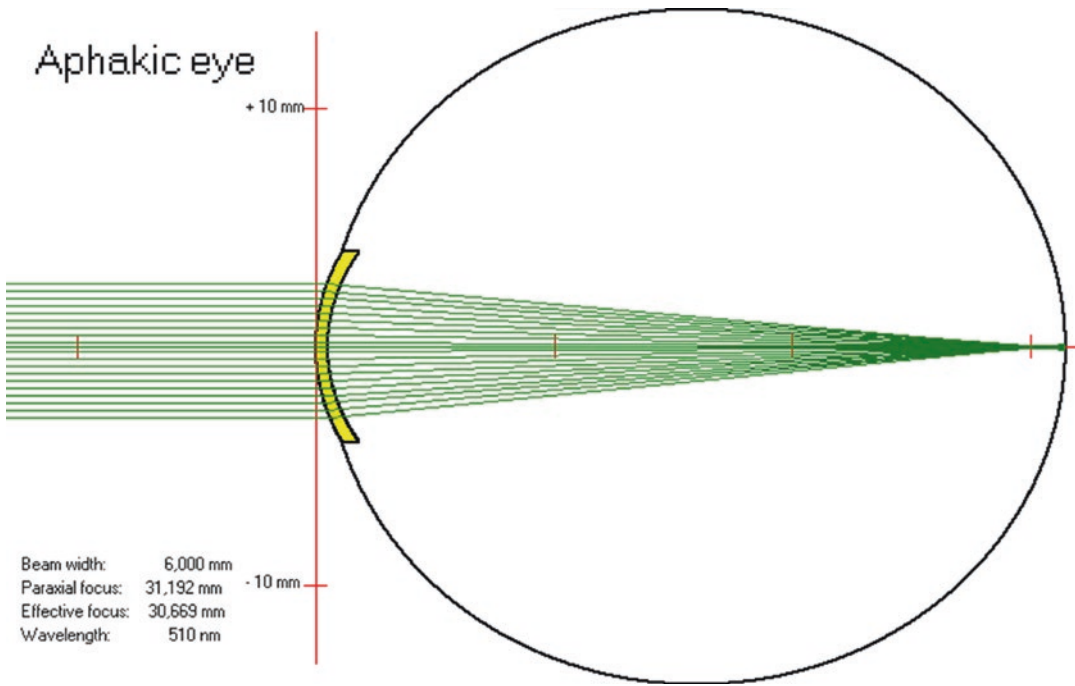


Fig. 14.4 Exact ray tracing of the cornea, simulated by a long, aphakic eye

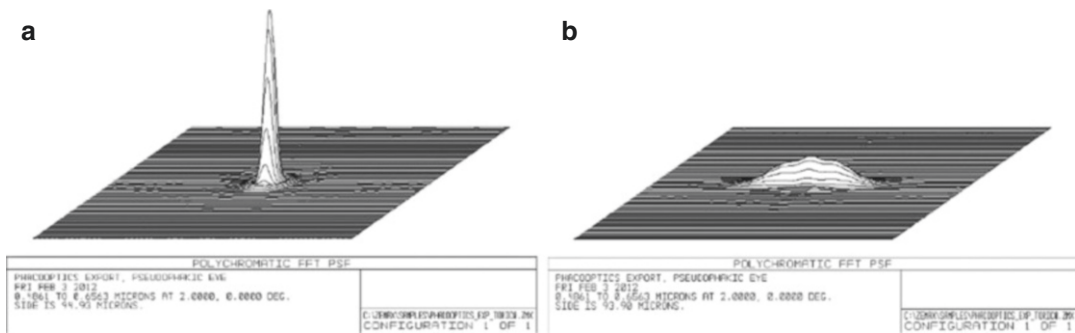


Fig. 14.5 Point spread function showing a good (a) and a bad (b) focus

the blur or point spread function observed at the focus. The blurring can be quantitated as the root-mean-square (RMS) of the ray intersections with the image plane around the axis. Figure 14.7 shows the RMS as a function of varying the front and back Q -values around the mean.

As can be seen from Fig. 14.7, the best image is found at zero spherical aberration which is found for a front corneal Q -value around -0.5 .

As the value for the normal cornea is around -0.18 , we see that there is room for improvement. The clinical tools to reduce spherical aberration of the IOL eye include: (1) altering the cornea profile toward more asphericity and (2) implant an aspheric IOL with a proper wavefront correction of the spherical aberration. It should be remembered; however, that an ultra-sharp, aberration-free focus comes at the expense of depth of focus.

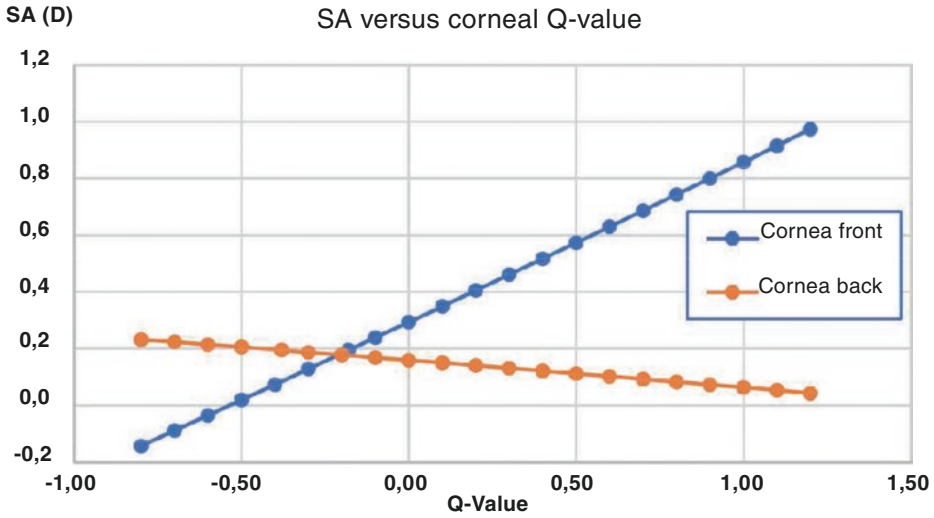


Fig. 14.6 The spherical aberration of the cornea is directly proportional to the Q -value of the front cornea. The posterior cornea has a much lower influence

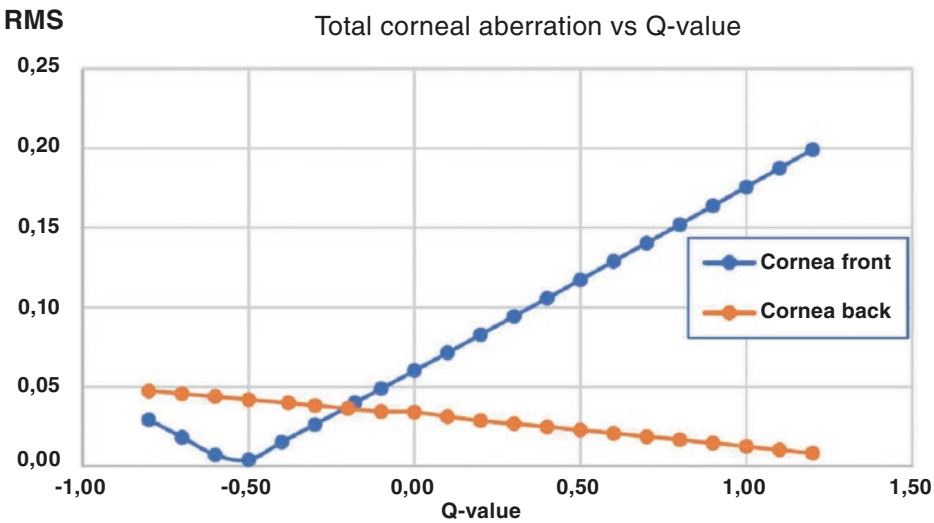


Fig. 14.7 Total corneal aberration as a function of front and back Q -value of the cornea

Clinical Studies Using Scheimpflug Data

As mentioned, exact ray tracing is an established technique often used in optical engineering to examine optical properties of any physical object. The advantage of the technique is that it does not use any assumptions on the shape of the surface if the surface is completely described in physical terms.

With the advent of modern scanning techniques (Scheimpflug, OCT) that measure both surfaces of the cornea in multiple points, we have an opportunity to study the optics of the cornea by exact ray tracing, which has obvious advantages over more assumptive methods. In the following, an example is shown of the steps involved in the calculation of the corneal power by ray tracing from raw matrix elevation data and how this compares with conventional methods [5].

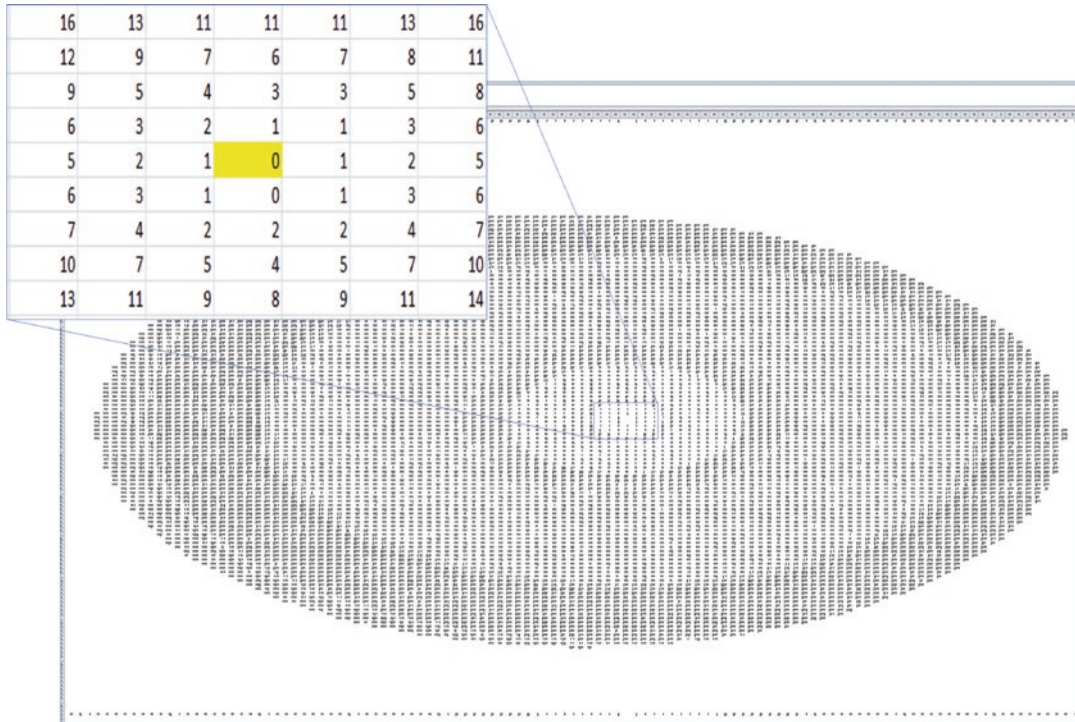


Fig. 14.8 A 3D matrix of mapped corneal data exported by the Oculus Pentacam HR ©. The Pentacam captures the height data in a (xy) matrix of a maximum of 140 ×

140 points of 0.1 mm interval. The insert shows the height (elevation) of the individual points in μm. The apex has an elevation of 0 μm (yellow point)

An example of the dataset exported by the Oculus Pentacam HR is shown in Fig. 14.8. The elevation data can be used to create a physical meshwork of individual points by a process called triangulation (Figs. 14.9 and 14.10). In this way, the cornea surface is represented by a continuous surface of minute triangles, which can be used by the ray tracing software.

An example of optical engineering software is the Zemax® program which has been used by the author to import the 3D triangulated dataset and analyze for refraction by ray tracing. A pupil can be inserted, and the effective focal length can be analyzed from a high number of rays refracted through the system. The focal distance is found as the point where the rays form the least blur and the highest point spread function (PSF) (Fig. 14.11). The effective power of the cornea is then found as the reciprocal of the effective focal distance.

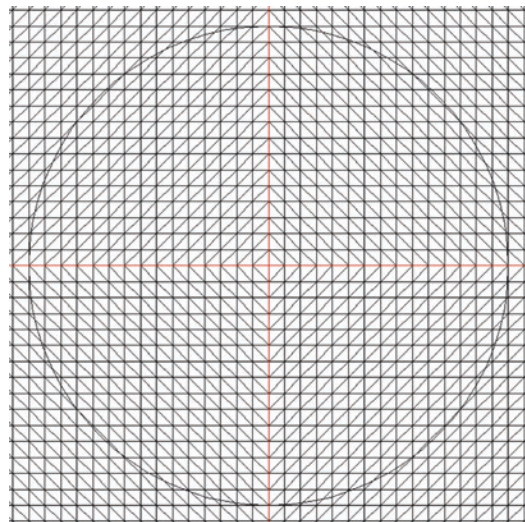


Fig. 14.9 This diagram is a front view of the triangulation around the vertex (0, 0). Each grid intersection represents a measurement point of a certain elevation in the Z-axis. The circle represents the pupil at a width of 3 mm

Fig. 14.10 Ray tracing through anterior and posterior cornea based on 3D elevation data exported by the Pentacam

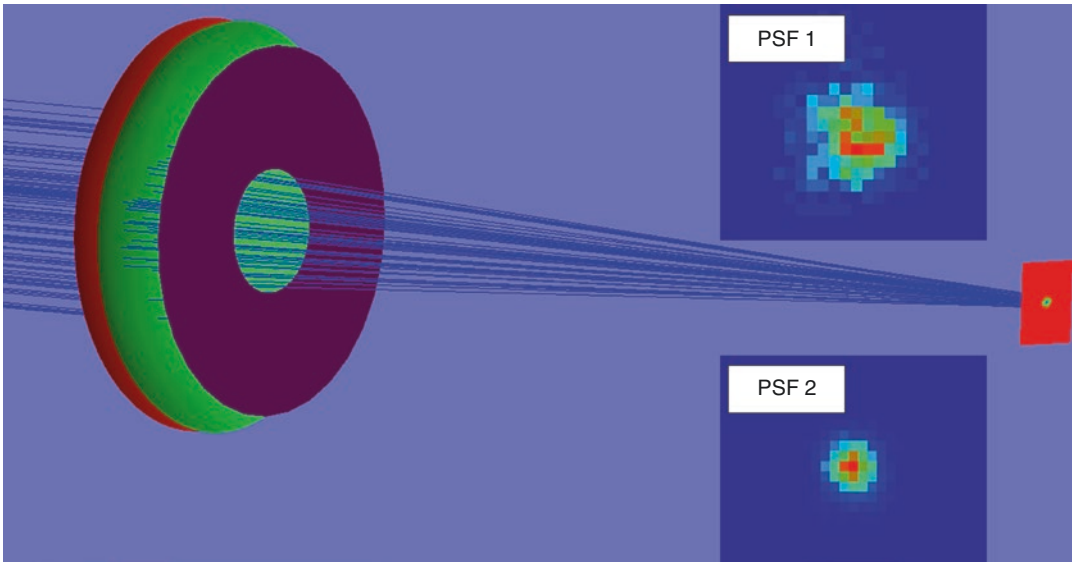
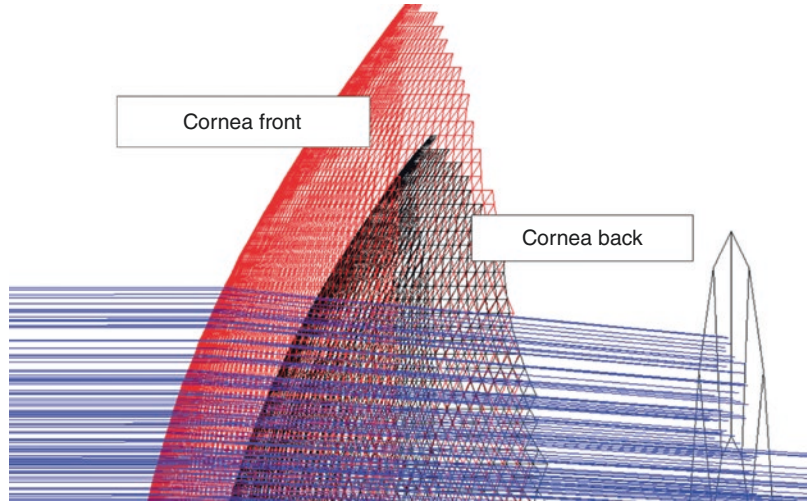


Fig. 14.11 The focal distance is found as the point where the rays form the least blur and the highest point spread function (PSF)

Table 14.2 shows the ray traced corneal power at different pupil sizes as compared to the Pentacam-derived True Net Power (TNP) and Total Corneal Refractive Power (TCRP) as well as the standard reading of the keratometer. The ray-traced corneal power is seen to increase as the pupil increases because of spherical aberration. The TNP gives the lowest value as this

value is calculated from the apical curvatures of the front and back surfaces of the cornea (paraxial domain) without the effect of the corneal asphericity. The standard K-reading is about 1 D higher than the ray-traced corneal power at 3 mm pupil.

You may ask the question: If keratometer index 1.3375 is bad, what is the best index

Table 14.2 Results of varying the pupil size on the estimated corneal power from ray tracing analysis of 20 normal subjects. The Pentacam variables “TNP” (“True Net Power,”

based on thick-lens calculation of the corneal power by the Pentacam software) and “TCRP” (“Total Corneal Refractive Power” based on an exact ray tracing algorithm)

N = 20	Zemax-derived corneal power (D)/pupil size			Pentacam variables (D)		Keratometer (D)
	3 mm	4 mm	5 mm	TNP	TCRP	“K-reading”
Mean (± SD)	42.34 (±1.33)	42.52 (±1.38)	42.64 (±1.41)	41.91 (±1.29)	42.38 (±1.28)	43.36 (±1.53)
Range	39.79–44.69	39.86–45.19	39.96–46.46	39.50–43.65	39.90–44.05	40.74–45.95

Table 14.3 Equivalent keratometer index that gives the same corneal power as the ray-traced value

Keratometric index (single surface equivalent)	Pupil 3 mm	Pupil 4 mm	Pupil 5 mm
Mean (±SD)	1.3207 (±0.0037)	1.3310 (±0.0041)	1.3320 (±0.0043)
Range	1.3165–1.3329	1.3165–1.3378	1.3170–1.3403

based on the ray tracing experiments? This value can be back-calculated in each case solving for the single-surface index giving the observed ray-traced corneal power. The results are shown in Table 14.3. As can be seen, the fictitious index for a 3 mm pupil was 1.3207 on average with a range from 1.3165 to 1.3329. The range actually includes the Gullstrand-derived value of 1.3315 as proposed by Olsen many years ago (see section “The Refractive Power of the Cornea” above). In other words, if one uses the Gullstrand ratio of 0.88 rather than the Scheimpflug-derived value of 0.83–0.84, then the corneal power includes the spherical aberration and may be regarded as the effective corneal power.

Figure 14.12 shows the comparison of K-reading, Pentacam Total Net Power (TNP) and Total Corneal Refractive Power (TCRP) versus the ray-traced corneal power assuming a 3 mm pupil in a large series of normal cataractous case ($n = 443$). The conventional K-reading gives the highest and the TNP the lowest value. There is remarkable good agreement between the TCRP and the ray-traced corneal power (regression coefficient 1.00 with no significant off-set and correlation coefficient $r = 0.99$).

Notes on the Stiles–Crawford Effect

These ray tracing calculations are valid from a purely optical point of view. However, the retina does not act like a simple screen. For many years, it has been known that the sensitivity of the retina is dependent on the incident angle of light on the retina. This directional sensitivity of the retina was discovered by Stiles and Crawford in 1933 [6] as a discrepancy between the objective and the effective area of the pupil in terms of luminous effectivity. The phenomenon predicts rays off axis to be less effective than central (paraxial) rays as a perceptive stimulus. The Stiles–Crawford equation is:

$$I = I_0 * e^{-0.108*y^2} \tag{14.8}$$

where I is stimulus efficacy of peripheral ray, I_0 efficacy of axial ray, y is distance of peripheral ray from axis. To correct for the Stiles–Crawford effect, we therefore put a weight on each ray according to this formula and solve for the best focus as described by Olsen in 1993 [7]. The result appears as the lower curve in Fig. 14.13. The Stiles–Crawford effect is insignificant in the normal area (pupil less than 4 mm). For a large pupil (8 mm), the effect amount to about 0.3 D less corneal power than predicted by optics alone.

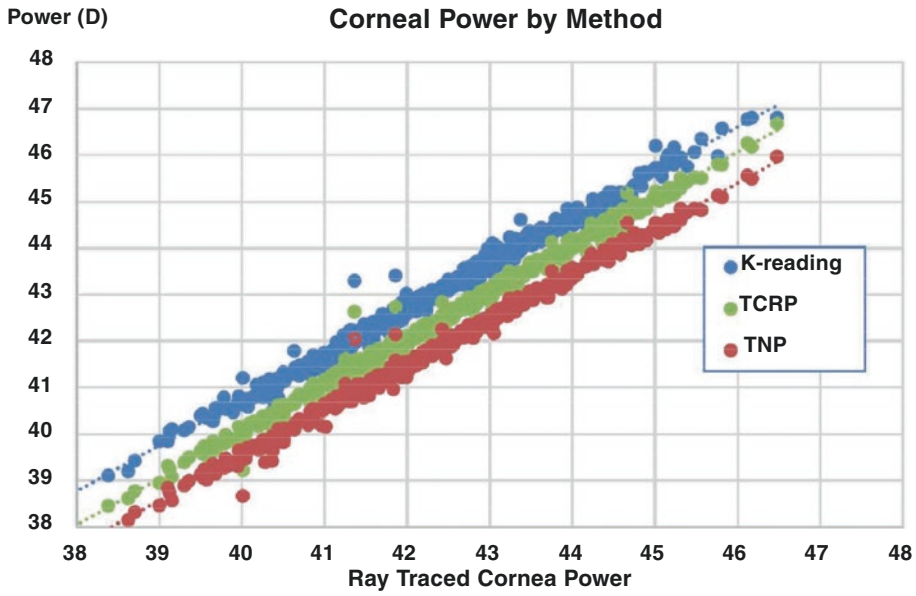


Fig. 14.12 The corneal power found by K-reading, Pentacam TNP, and TCRP versus the ray-traced power based on mapped elevation data assuming a 3 mm pupil ($n = 443$ normal cases)

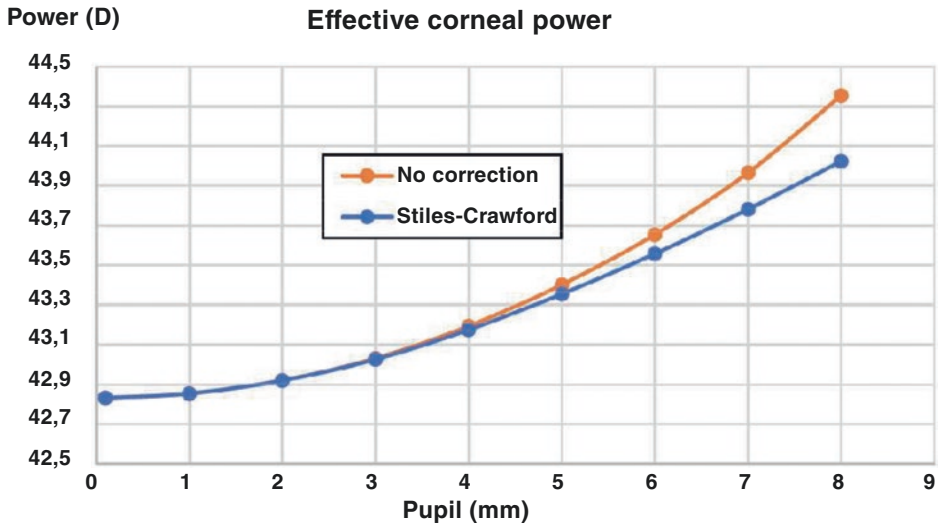


Fig. 14.13 The effective corneal power as a function of pupil size

References

1. Bennett AG, Rabbetts RB. What radius does the conventional keratometer measure? *Ophthal Physiol Opt.* 1991;11(3):239–47.
2. Gullstrand A. Einführung in die Methoden der Dioptrik des Auges des Menschen. In: Helmholtz H, editor. *Handbuch der physiologischen Optik des Auges.* Leipzig: Verlag von S. Hirzel; 1911. p. 152.
3. Dubbelman M, Weeber HA, van der Heijde RG, Volker-Dieben HJ. Radius and asphericity of the posterior corneal surface determined by corrected Scheimpflug photography. *Acta Ophthalmol Scand.* 2002;80:379–83.
4. Baker TY. Ray tracing through non-spherical surfaces. *Proc Phys Soc.* 1943;55:361–4.
5. Olsen T, Jeppesen P. Ray-tracing analysis of the corneal power from Scheimpflug data. *J Refract Surg.* 2018;34(1):45–50.
6. Stiles WS, Crawford BH. The luminous effectivity of rays entering the eye pupil at different points. *Proc R Soc Lond.* 1933;112:428–50.
7. Olsen T. On the Stiles-Crawford effect on ocular imagery. *Acta Ophthalmol Scand.* 1993;71:85–8.

Open Access This chapter is licensed under the terms of the Creative Commons Attribution 4.0 International License (<http://creativecommons.org/licenses/by/4.0/>), which permits use, sharing, adaptation, distribution and reproduction in any medium or format, as long as you give appropriate credit to the original author(s) and the source, provide a link to the Creative Commons license and indicate if changes were made.

The images or other third party material in this chapter are included in the chapter's Creative Commons license, unless indicated otherwise in a credit line to the material. If material is not included in the chapter's Creative Commons license and your intended use is not permitted by statutory regulation or exceeds the permitted use, you will need to obtain permission directly from the copyright holder.

